

Abstract

Past and current gravimetric satellite missions have contributed drastically to our knowledge of the Earth's gravity field. Nevertheless, several geoscience disciplines push for even higher requirements on accuracy, homogeneity and time- and space-resolution of the Earth's gravity field. Apart from better instruments or new observables, alternative satellite formations could improve the signal and error structure. With respect to other methods, one significant advantage of the semi-analytical approach is its effective pre-mission error assessment.

The semi-analytical approach builds a linear analytical relationship between the Fourier spectrum of the observables and the spherical harmonic spectrum of the gravity field. The spectral link between observables and gravity field parameters is given by the transfer coefficients, which constitute the observation model. In connection with a stochastic model, it can be used for pre-mission error assessment of gravity field missions.

The cartwheel formation is formed by two satellites on elliptic orbits in the same plane. The time dependent ranging is considered in the transfer coefficients via convolution. The transfer coefficients are applied to assess the error patterns, which are caused by different orientation of the cartwheel for range-acceleration. The formal errors and isotropy are presented for different orientations of the cartwheel.

1. The semi-analytical approach

The semi-analytical approach enables the prediction of formal errors of the recovered gravity model based on satellite observables in space. Figure 1 illustrates the scheme of the semi-analytical approach. The design matrix A is filled by the transfer coefficients $H_{lmk}^\#$, which are calculated from the nominal orbital parameters:

- h : orbit height,
- I : inclination,
- ω_0 : initial argument of perigee, ...

and the type of observables (without data). Inversion of the normal matrix separately for each order m and even/odd separation for degree l and order k provide the formal error σ_{lm} of the gravity field due to the satellite formation.

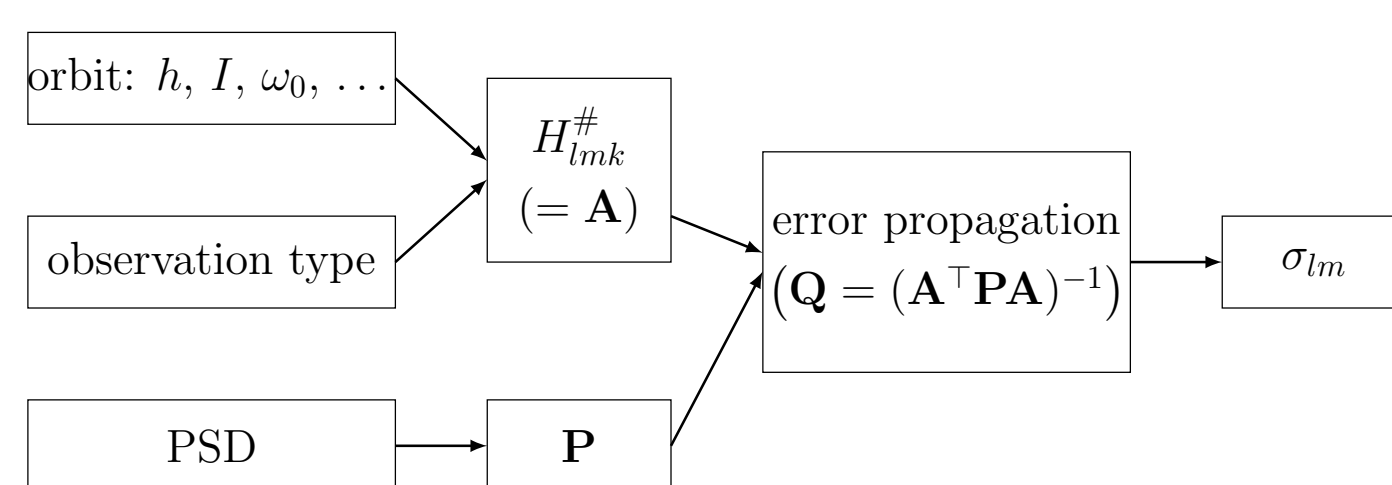


Figure 1: Concept of the semi-analytical approach.

For the semi-analytical approach, the observations must be expressed in the rotating local triad, where x -axis is pointing towards the satellite and the z -axis is perpendicular to the orbital plane. In this system, for the eccentric nominal orbit, the along-orbit gravitational potential can be presented as time series:

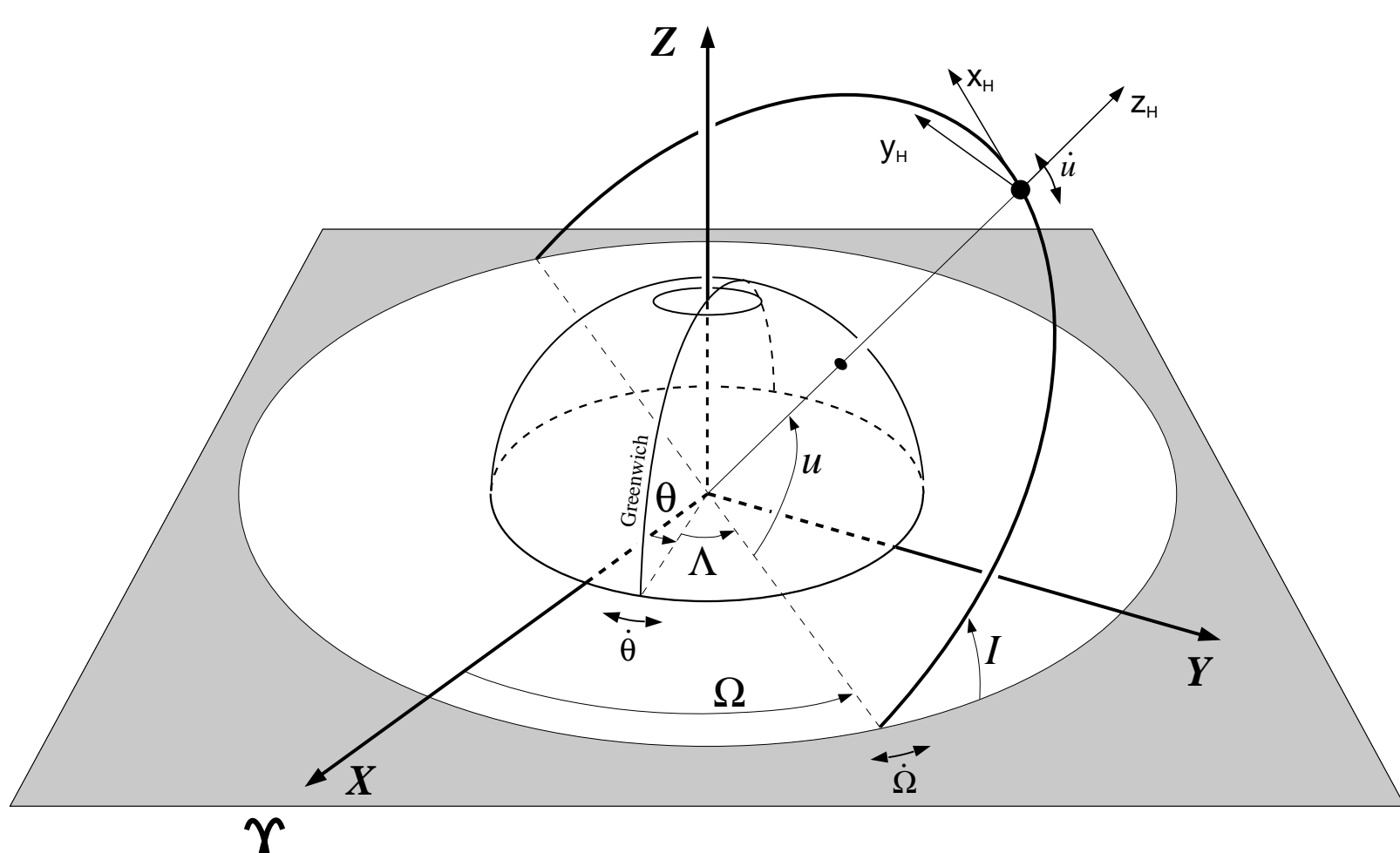


Figure 2: Nominal orbit configuration

$$V = \frac{GM}{R} \sum_{l=0}^{\infty} \left(\frac{R}{a}\right)^{l+1} \sum_{m=-l}^l \sum_{k=-l}^l \sum_{q=-\infty}^{\infty} \bar{K}_{lm} \bar{F}_{lmk}(I) G_{lkq}(e) e^{i\psi_{mkq}}, \quad (1)$$

with

$$\psi_{mkq} = k\omega + (k+q)M + m\Lambda = k\omega + k^*M + m\Lambda, \quad k^* = k+q.$$

In the above formula, $\bar{F}_{lmk}(I)$ is the complex inclination function, and $G_{lkq}(e)$ is the eccentric function. In this work, we don't consider the procession of perigee. Not only the potential, but also its functionals $f^\#$, in which the label $\#$ represents a specific observable, can be represented by 2D Fourier series [1].

$$f^\# = \sum_{m=-\infty}^{\infty} \sum_{k^*=-\infty}^{\infty} A_{mk^*}^\# e^{i\psi_{mk^*}} \quad (2)$$

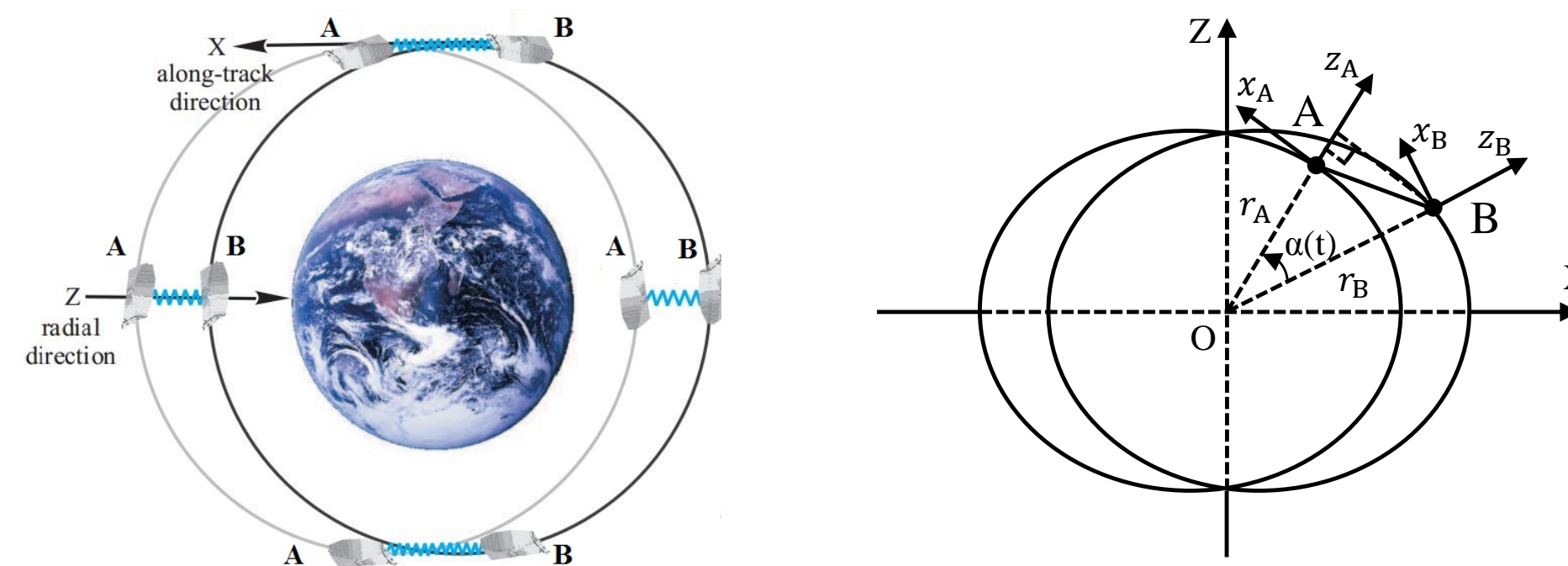
$$A_{mk^*}^\# = \sum_{q=-\infty}^{\infty} \sum_{l=\max(|m|, |k|)}^{\infty} H_{lmk^*-q}^\# \bar{K}_{lm},$$

with the transfer coefficients $H_{lmk}^\#$. The formal errors of \bar{K}_{lm} are found by error propagation $D\{\hat{x}\} = (A^T P A)^{-1}$.

2. Transfer coefficients for the cartwheel formation

2.1 Cartwheel formation

In the cartwheel formation, ranging measurements are observed between two satellites on two elliptic orbits in the same plane, with a 180° separation in perigee. In comparison to GRACE, the observation contains components in along-track and radial directions depending on the time-dependent central angle α .



(a) formation in space [2] (b) relative orientation

Figure 3: Cartwheel formation with $\omega_0 = 0^\circ$ (the radial direction is at the equator)

The cartwheel formation can be described by relative motion of two satellites in the Hill-frame by means of the homogeneous solution of the Hill equations as

$$\begin{aligned} \rho_x(t) &= -2\rho_r \sin(\dot{u}t - \omega_0) \\ \rho_y(t) &= 0 \\ \rho_z(t) &= \rho_r \cos(\dot{u}t - \omega_0). \end{aligned} \quad (3)$$

In Figure 3(b), A and B are satellites of the cartwheel formation and satellite A is set as the reference point. So the perturbations of satellite B, $\vec{\Delta}_B = (\Delta x_B, \Delta y_B, \Delta z_B)^\top$ in B-Hill frame have to be rotated into A-Hill frame around y -axis by α , yielding to:

$$\vec{\Delta}_B' = \mathbf{R} \cdot \vec{\Delta}_B = (\Delta x_B', \Delta y_B', \Delta z_B')^\top, \quad (4)$$

According to formula (3), we know the unit vector of baseline in A-Hill frame is,

$$\vec{e}_A = \frac{\vec{AB}}{|\vec{AB}|} = \frac{(-2\rho_r \sin(nt - \omega_0), 0, \rho_r \cos(nt - \omega_0))^\top}{\sqrt{\rho_r^2 + 3\rho_r^2 \sin^2(\dot{u}t - \omega_0)}}$$

So the contributions of satellites A and B to the perturbation of baseline are

$$\Delta\rho = \Delta\rho_A + \Delta\rho_B = -\vec{e}_A \cdot \vec{\Delta}_A + \vec{e}_A \cdot \vec{\Delta}_B.$$

Then we can get the final expression of the perturbation of range:

$$\begin{aligned} \Delta\rho &= \frac{2 \sin(\dot{u}t - \omega_0)}{\sqrt{1+3 \sin^2(\dot{u}t - \omega_0)}} \Delta x_A + \frac{-\cos(\dot{u}t - \omega_0)}{\sqrt{1+3 \sin^2(\dot{u}t - \omega_0)}} \Delta z_A \\ &+ \frac{\cos(\dot{u}t - \omega_0) \sin \alpha - 2 \sin(\dot{u}t - \omega_0) \cos \alpha}{\sqrt{1+3 \sin^2(\dot{u}t - \omega_0)}} \Delta x_B \\ &+ \frac{2 \sin(\dot{u}t - \omega_0) \sin \alpha + \cos(\dot{u}t - \omega_0) \cos \alpha}{\sqrt{1+3 \sin^2(\dot{u}t - \omega_0)}} \Delta z_B \end{aligned} \quad (5)$$

2.2 Transfer coefficients for cartwheel

Satellite A and B have different arguments of perigee and mean anomalies, and both of the differences are π . Here we set the argument of perigee of satellite A as ω_0 . The choice $\omega_0 = 0^\circ$ means that the cartwheel orientation is radial at the equator and along-track at the poles, and $\omega_0 = 90^\circ$ means that along-track is at the equator and radial is at the poles. So the perturbation in x -direction can be expressed as:

$$\begin{aligned} \Delta x_A &= \sum_{l,m,k^*} \sum_{q=-Q}^Q H_{l,m,k^*-q}^{\Delta x} G_{l+1,k^*-q,q} e^{ik^*\omega_0} \bar{K}_{lm} e^{i\psi_{mk^*}} \\ \Delta x_B &= \sum_{l,m,k^*} \sum_{q=-Q}^Q H_{l,m,k^*-q}^{\Delta x} G_{l+1,k^*-q,q} e^{ik^*\omega_0} (-1)^q \bar{K}_{lm} e^{i\psi_{mk^*}} \end{aligned} \quad (6)$$

with $k^* = k+q$. The factor $(-1)^q$ in the term Δx_B is introduced by the difference of argument of perigee between these two satellites. The perturbations in z -direction can be derived analytically in the similar way. Similar to the pendulum formation, the time dependent orbital elements (in the gray boxes) can be expanded as Fourier series with the orbit frequency as base frequency:

$$\begin{aligned} \frac{2 \sin(\dot{u}t - \omega_0)}{\sqrt{1+3 \sin^2(\dot{u}t - \omega_0)}} &= \sum_{n=-N}^N A_n e^{in\dot{u}t} \\ \frac{-\cos(\dot{u}t - \omega_0)}{\sqrt{1+3 \sin^2(\dot{u}t - \omega_0)}} &= \sum_{n=-N}^N B_n e^{in\dot{u}t} \\ \frac{\cos(\dot{u}t - \omega_0) \sin(2\alpha) - 2 \sin(\dot{u}t - \omega_0) \cos(2\alpha)}{\sqrt{1+3 \sin^2(\dot{u}t - \omega_0)}} &= \sum_{n=-N}^N C_n e^{in\dot{u}t} \\ \frac{2 \sin(\dot{u}t - \omega_0) \sin(2\alpha) + \cos(\dot{u}t - \omega_0) \cos(2\alpha)}{\sqrt{1+3 \sin^2(\dot{u}t - \omega_0)}} &= \sum_{n=-N}^N D_n e^{in\dot{u}t} \end{aligned} \quad (7)$$

Substituting formula (5) and (6) into range perturbation formula (5) results in the final transfer coefficients:

$$\begin{aligned} H_{lmk}^{\Delta\rho} &= \sum_{q=-Q}^Q \sum_{n=-N}^N (H_{l,m,k'-n-q,q}^{\Delta x_A} A_n + H_{l,m,k'-n-q,q}^{\Delta z_A} B_n) \\ &+ \sum_{q=-Q}^Q \sum_{n=-N}^N (H_{l,m,k'-n-q,q}^{\Delta x_B} C_n + H_{l,m,k'-n-q,q}^{\Delta z_B} D_n) \end{aligned}$$

with $k' = k^* + n = k + q + n$.

3. Simulations

In our simulation, the semi-analytical approach is performed for a semi-major axis $a = 335$ km, $\rho_r = 50$ km, $\rho_x = 100$ km, and inclination of 90° . The white noise $10^{-10} \text{ s}^2 \sqrt{\text{Hz}}$ and realistic noise models based on the model of NGGM [3] are used on for the simulations, respectively. The formal error and spatial covariance functions are presented for radial direction at the equator ($\omega_0 = 0^\circ$) and at the poles ($\omega_0 = 90^\circ$), respectively.

Formal errors

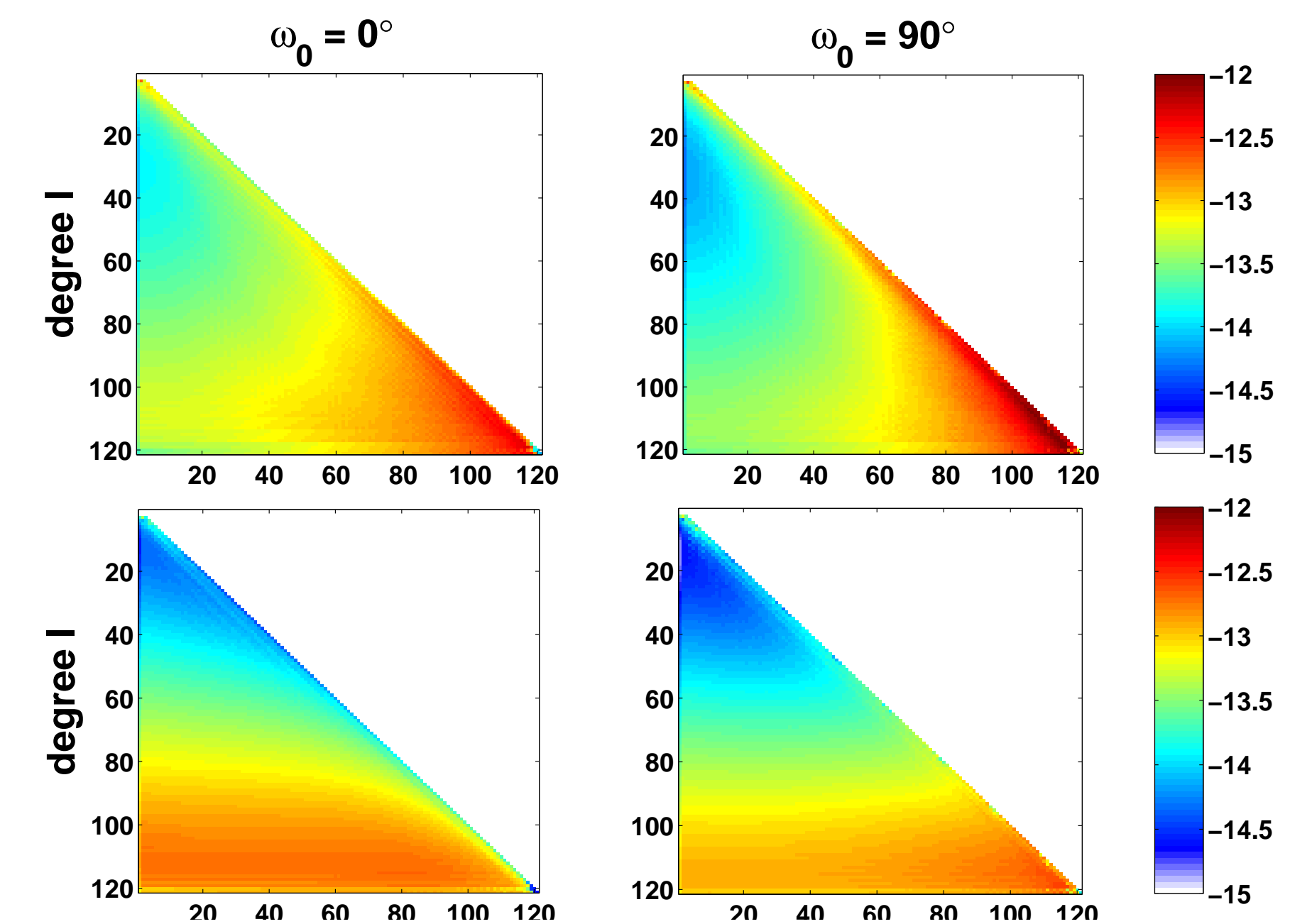


Figure 4: Formal error $[\log_{10}]$ for white noise (up) and colored noise (down)

Spatial covariance functions $[\text{m}^2]$ at $\phi = 0^\circ$

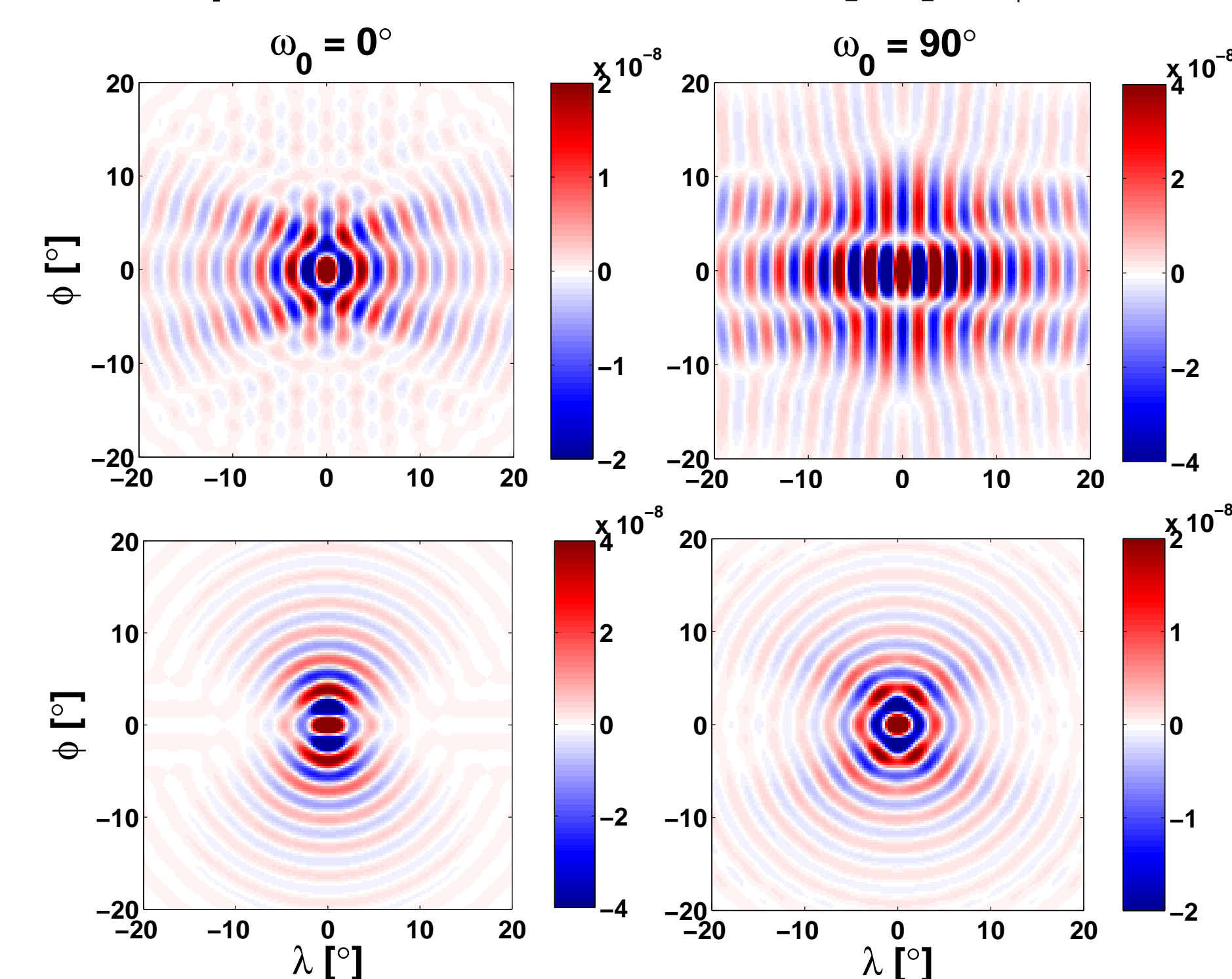


Figure 5: Spatial covariance functions for white noise (up) and colored noise (down)

4. Conclusions

From the results, we can see that for the white noise, the formal error level for $\omega_0 = 90^\circ$ is better, but for the isotropy, the $\omega_0 = 0^\circ$ case is better. For the colored noise case, the formal error level is lower for $\omega_0 = 90^\circ$. At the same time, the argument of perigee of 90° case also leads to the more isotropic solution in spatial domain. Since we didn't consider the procession of perigee, the results for other perigee cases should be between these extreme two cases ($\omega_0 = 0^\circ$ and $\omega_0 = 90^\circ$).

References

- [1] N. Sneeuw 2000: A semi-analytical approach to gravity field analysis from satellite observations, Dissertation, Technische Universität München, DGK.
- [2] B. Elsaka 2010: Simulated satellite formation flights for detecting the temporal variations of the Earth's gravity field, Dissertation, Universität of Bonn.
- [3] T. Gruber and NGGM team 2014: e2.motion: Earth System Mass Transport Mission (Square) - Concept for a Next Generation Gravity Field Mission - Final Report of Project Satellite Gravimetry of the Next Generation (NGGM-D). DGK, Reihe B Nr. 318, München.